JMEPEG (2010) 19:633–642
DOI: 10.1007/s11665-009-9522-7

1059-9495/$19.00

Study on Hot Ring Compression Test of Nimonic 115 Superalloy Using Experimental Observations and 3D FEM Simulation

D. Shahriari, A. Amiri, and M.H. Sadeghi

(Submitted December 5, 2008; in revised form June 23, 2009)

In hot forging of Nimonic 115, it is desirable to determine friction coefficients. Changing magnitudes of temperature and type of lubricant at the surface of the workpiece and dies influence friction coefficient. This paper describes an experimental investigation of friction under hot forging conditions using the ring compression test. The 3D FEM simulations were used to derive the friction calibration curves and to evaluate material deformation, geometric changes, and load-displacement results. A series of ring compression tests were carried out to obtain friction coefficients for a number of lubricants including mica plate, glass powder, graphite powder, and dry condition. The experiments show how the variations in temperature at the interface affected frictional behavior. On the basis of these results, mica is recommended for hot forging of Nimonic 115 and its friction coefficient is approximately 0.3.

Keywords friction coefficient, hot forging, Nimonic 115, ring test

1. Introduction

The nickel-based superalloys are most widely used in a variety of high performance applications, at temperatures ranging from 650 to 1050 °C in aggressive atmospheres (Ref 1, 2). Nimonic series of superalloys are nickel-chromium alloys which are strengthened by additions of titanium and aluminum. The Nimonic alloys possess a superior high-temperature creep and oxidation resistance and are used for high temperature, high strength applications, such as gas turbine hot section components, for hot work tools and forging hammers (Ref 1-3). Friction between the workpiece and the tooling plays an important role in many bulk forming processes such as forging, extrusion, and rolling. Metal flow patterns and the generation of defects can be strongly influenced by frictional conditions. As such, several methods have been developed to quantify interface friction. The ring compression test was developed to provide a measurement of the interface friction between the workpiece and dies, but it also can be used to provide reasonable values for the flow stress in compression. In the ring compression test, when a flat ring specimen is compressed between two flat platens, increasing friction results in an inward flow of the material, while decreasing friction results in an outward flow of the material as schematically illustrated in Fig. 1 (Ref 4, 5). For a given percentage of height reduction during compression tests, the corresponding measurement of the internal diameter of the test specimen provides a quantitative knowledge of the magnitude of the prevailing friction coefficient at the die-workpiece interface. If the specimen's internal diameter increases during the deformation, friction is low; if the specimen's internal diameter decreases during the deformation, the friction is high. Male (Ref 6) carried out a study in order to obtain variations in the friction coefficient of metals during compressive deformation at room temperature. His results showed that the coefficient of friction tended to increase with an increasing deformation rate for different metals under dry conditions and with a solid lubricant. Male (Ref 7) showed that the coefficient of friction μ changes with temperature. As the temperature increased, it was observed that μ may increase to full sticking friction or it may even decrease depending on the material of the ring. Jain and Bramely (Ref 8) have made a detailed investigation of the relations between the coefficient of friction and the forging speed using the ring test at the constant temperature of 1120 °C. Using various lubricants, it was concluded that in all cases, as the impact speed increased the frictional coefficient would be reduced.

Male et al. (Ref 9) conducted a research study in order to see which one more realistically defines the friction condition in the metal-forming processes. They showed that *m* as a quantitative index for defining friction conditions in upset forging operations was more realistic than μ which underestimated frictional components of the deformation load. It was also found that the ring compression test is an accurate technique to determine the true stress-true strain curve in typical metal-forming operations, and its accuracy was shown at high temperatures and low strain rates. Felder and Montagut (Ref 10) carried out ring compression tests at 1250 °C. They discovered that the tool velocity had a significant effect on friction, and it was shown that the friction decreases if the velocity increases.

D. Shahriari, Manufacturing Group, Department of Mechanical Engineering, Faculty of Engineering, Tarbiat Modares University, P.O. Box 14115-143, Tehran, Iran; and Mapna Group (MavadKaran Eng. Co.), P.O. Box 13445-556, Tehran, Iran; and **A. Amiri** and **M.H. Sadeghi**, Manufacturing Group, Department of Mechanical Engineering, Faculty of Engineering, Tarbiat Modares University, P.O. Box 14115-143, Tehran, Iran. Contact e-mails: Da_Shahriari@yahoo.com, Da_Shahriari@modares.ac.ir, Amiri@modares.ac.ir, Sadeghim@modares.ac.ir. URLs: www.modares.ac.ir and www.mavadkaran.com.

Pawelski et al. (Ref 11) considered the effect of the ring material, scale, lubricant, reduction, strain rate, and temperature on the resulting changes of geometry and the corresponding shear factor. They concluded that for unlubricated specimens, the strain rate and temperature had no effect on the shear factor, "*m*." Specimens which had a lubricant applied showed that increasing strain rate caused the shear factor "*m*" to reduce. Increasing the temperature caused an increase in the shear factor.

Venugopal et al. (Ref 12) compressed unlubricated ring specimens made of Armco iron and concluded that varying the temperature between 30 and 1000 °C did not have a significant effect on the magnitude of the shear factor "*m*." Sadeghi and Dean (Ref 13) investigated the effect of temperature on friction using the ring compression test. The tests were carried out using steel specimens with a graphite-based lubricant. It was shown that in the temperature range of 700-1150 °C, the magnitude of the shear factor "*m*" increased with increasing temperature. Ring calibration curves are dependent upon the strain rate sensitivity as well as the ring geometry (Ref 14). Wang and Lenard (Ref 15) studied interfacial friction on the hot ring compression test in which the strain rate and temperature were identified as the significant factors affecting the frictional shear factor at the interface of the die-workpiece. At true strain rates 0.005-5 s^{-1} in the temperature range of 900-975 °C using a glass-based lubricant, the experiments showed that the shear factor "*m*" dropped from 0.35 to 0.1 with increasing strain rate. Rudkins et al. (Ref 16) showed that for steel specimens, increasing the temperature causes the level of friction to increase. Sofuoglu and Rasty (Ref 17) recommended although the ring compression test is an effective method for determining the coefficient of friction during large deformation processes, the use of a generalized friction calibration chart regardless of the material type and test conditions must be avoided. Lee et al. (Ref 18) investigated the influence of die velocity on the friction factor for aluminum and bronze, and showed the friction factor decreases when the die velocity is increased. Hence, there is a need to determine calibration curves, estimating the friction factor and suitable lubricant for hot forging of nickel base superalloys at various high temperatures. This study proposes an efficient and systematic method to derive calibration curves for friction between the dies and a workpiece by means of finite element method simulations that incorporate the effect of variations in temperature on material flow and to establish the specific friction factors that pertain to various experimental lubrication conditions at different temperatures for Nimonic 115.

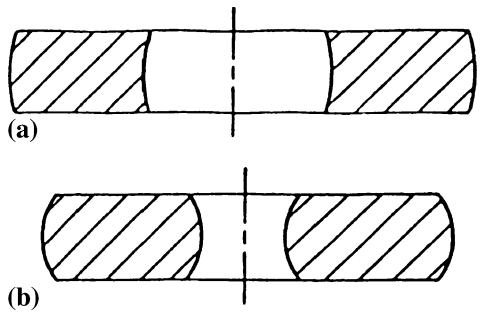

Fig. 1 Variation in shape of ring test specimens deformed the same amount under different frictional conditions. (a) Low friction and (b) high friction

2. Rigid Viscoplastic Finite Element Formulation

FEM simulation has been used to simulate hot deformation processes including the hot ring test (Ref 4, 5, 16, 19-24). In these formulations, a heat transfer model is also coupled to the material model to account for the thermomechanical effects (Ref 5, 16, 19-21). In this study, an in house FEM code based on an updated Lagrangian description using a rigid viscoplastic material formulation coupled with a heat transfer formulation was employed to simulate the hot ring test process. This approach is in line with those reported by other workers and allows to take into account the thermomechanical history of the workpiece. The governing equations for solving the rigid viscoplastic material can be found in the following references (Ref 4, 5, 16, 19-21) and only the major equation used in the FEM formulation is provided below:

$$\delta\pi = \int_V \bar{\sigma}\,\delta\dot{\bar{\varepsilon}}dV + K\int_V \dot{\varepsilon}_V\delta\dot{\varepsilon}_V dV - \int_{S_F} F_i\delta u_i dS = 0 \quad \text{(Eq 1)}$$

where $\bar{\sigma}$ is the effective stress, $\dot{\bar{\varepsilon}}$ is the effective strain rate, $\dot{\varepsilon}_v$ is the volumetric strain rate. F_i represents surface tractions and K, a penalty constant, is a very large positive constant.

For problems such as ring compression, rolling, and forging, the unknown direction of the relative velocity between the die-workpiece interfaces make it difficult to predict the condition of constant frictional stress. Hence, a velocity dependent frictional stress is used as an approximation and at the interface, the velocity boundary condition is given in the direction normal to the interface by the die velocity (Ref 4, 5, 16, 19-23). Under these conditions, the traction boundary condition is expressed by:

$$f_S = mkL = mk\left\{\frac{2}{\pi}\tan^{-1}\left(\frac{|u_S|}{u_0}\right)\right\}\frac{u_S}{|u_S|} \quad \text{(Eq 2)}$$

where f_S is the frictional stress, m the friction factor, k the yield shear stress, L the unit vector in the opposite direction of the relative sliding velocity, u_S the sliding velocity of the work piece relative to the die, and u_0 a small positive number compared with u_S. Thus, the finite element discretization procedure is based on Eq 1 and 2 in mind for the die-workpiece interface boundary condition.

When deformation takes place at high temperatures, material properties can vary considerably with temperature. In fact, at elevated temperatures, plastic deformation can induce phase transformations and may result in the occurrence of recrystallization (static, dynamic, and metadynamic) which modify grain size and morphology. These microstructural changes affect significantly the flow stress of the material as well as its other mechanical properties. To consider these effects in this study, it was assumed that the rigid viscoplastic material is coupled with heat transfer analysis by the energy balance equation, expressed as:

$$k_1 T_{,ii} + \dot{r} - \rho c\dot{T} = 0 \quad \text{(Eq 3)}$$

K_1 denotes thermal conductivity, $\dot{r}$ is the heat generation rate, and $\rho c\dot{T}$ is the internal energy rate.

Solving the above equations by assuming that the heat generated during the deformation of workpiece is only due to plastic deformation, the temperature distribution of the workpiece and dies can be obtained. However, due to the nonlinearity involved in material properties, coupled with

thermal problem and frictional contact conditions, the solution to the above equation is very complex and in this study an iterative approach was used to obtain the solution.

3. Friction Modeling

Friction models normally applied in finite element analyses for bulk metal forming are the following:

3.1 Coulomb Friction Model

Amonton's law is one of this friction model usually adopted in finite-element computer programs that can be expressed as follow:

$$\tau = \mu P \qquad \text{(Eq 4)}$$

This law is valid for elastic contacts as well as for forming processes with low interfacial pressures. In the simulation of bulk metal-forming processes, the use of Amonton's law gives occasion for an over-estimation of the friction stresses at the die-workpiece interface, because the normal pressure often reaches values considerably greater than the flow stress of the material (Ref 4, 5, 19, 23). Consequently, the friction stress becomes greater than the flow stress of the material in pure shear.

3.2 The Constant Friction Model

The constant friction law, which is useful at high pressures, is stated as below:

$$\tau = mk \qquad \text{(Eq 5)}$$

where "m" is the frictional shear factor, which has a value "$m = 0$" for a frictionless interface and "$m = 1$" for sticking friction. This has great mathematical convenience because τ is defined with the aid of k, the value of which is known from the outset. In contrast, the use of μ can lead to complications because the value of P has to be found. As discussed in Avitzur's work (Ref 19-23), an average Coulomb friction coefficient, μ, may be calculated for measured "m" friction factors using the relation:

$$k = \frac{\sigma_0}{\sqrt{3}} \qquad \text{(Eq 6)}$$

$$\mu = \frac{m}{\sqrt{3}}\left(\frac{\sigma_0}{P_{ave}}\right) \qquad \text{(Eq 7)}$$

Avitzur also obtained the relation expressed in Eq 8, which gives the average surface pressure (P_{ave}) required to deform solid cylindrical specimens of diameter, d.

$$\frac{P_{ave}}{\sigma_0} = 1 + \frac{2m}{3\sqrt{3}}\left(\frac{d}{h}\right) \qquad \text{(Eq 8)}$$

3.3 The General Friction Model

The general friction model, which is a combination of two models mentioned above, is given by the following relationship:

$$\tau = f \alpha k \qquad \text{(Eq 9)}$$

The friction coefficient (μ) or shear friction factors (m and f) are employed as the dimensionless numbers for similarity in frictional conditions.

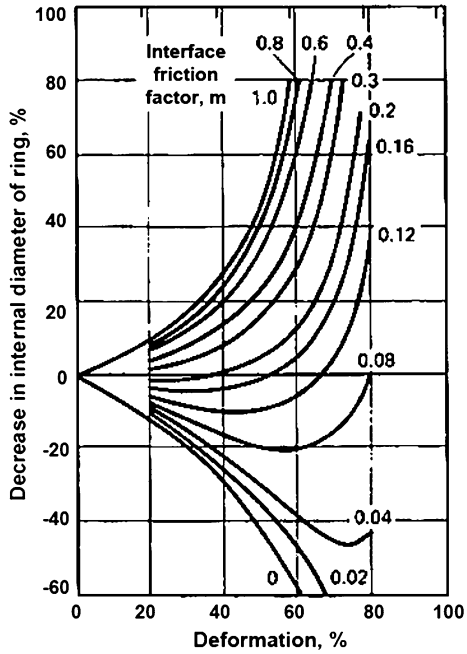

Fig. 2 Theoretical calibration curve for standard ring with an OD:ID:thickness ratio of 6:3:2

The Wanheim-Bay general friction model assumes friction to be proportional to the normal stress at low normal pressure $P/\sigma_0 \prec 1.5$ and going toward a constant value at high normal pressure $P/\sigma_0 \succ 3$. Using analytical methods, different sets of curves called calibration curves are obtained to determine the values of "m" or "f" for a specific lubricant. The shape of these curves is mainly influenced by the initial geometry of the ring used in the analysis (Ref 21). The calibration curves for m are like those shown in Fig. 2. The main objective of the present investigation is to find appropriate model lubricants and frictional conditions for hot metal forging processes with Nimonic 115 as the model material.

4. Influence of Lubricants

The lubrication processes can take many different forms, depending on the geometry of the contacting bodies, the roughness and texture of the sliding surfaces, the contacting load, the pressure and temperature, the rolling and sliding speeds, the environmental conditions, the physical and chemical properties of the lubricant, the material composition, and the properties of the near-surface layer (Ref 21-24). The choice of lubricant depends on the processing conditions, the characteristics of the tooling and work piece, and the operating or interfacial temperature, with the latter probably having the greatest influence on the lubricant selection. The frequency of application of the lubricant depends directly on the temperature, size and complexity of the die, and the frequency of the forging operation. The operating temperature has the greatest influence on the lubricant selection. At low temperatures, teflon- and graphite-based lubricants are adequate for most purposes, but at higher temperatures glass-based lubricants are often used. There is some overlap in the operating temperature ranges for the different lubricant types and often a number of different

Table 1 Summary of suggested workpiece-tooling-lubricant combinations

Workpiece	Temperature range, °C	Lubrication	Tooling
Al alloys	RT-liquidus	Glass	Al_2O_3, Glass, Mo
	200-450	Graphite	H13 Tool steel
	300-400	Graphite	Quartz
	<350	Teflon	Tool steel
	350-600	Water-based graphite	Tool steel
	400-450	Tallow grease	H13 Tool steel
	400-450	Synthetic oil	H13 Tool steel
	<400	PTFE dry lubricant	Inco 718
	450-550	Graphite foil	WC
	Ambient-550	Graphite in water	Inco 718
Fe alloys	RT-1500	Glass, graphite foil	Al_2O_3, Mo
	>800	Glass	Tool steel
	750-1200	Graphite foil, BN	M22, Sialon
	1100	Acheson DPG 3479 Glass/styrene acrylic	Sialon, Maraging Steel
	850-1100	Water and light oil	Chill cast iron, Chromium alloy steel
800-1300	Graphite foil	WC+ Ta/Ni Foil	
Ni alloys	850-1150	Borate glass + BN graphite + glass + BN	Inconel M22B TZM molybdenum
	800-1050	Graphite-Achesons Deltaglaze 3418	Mar M246
	1100	Acheson DPG 3479 glass/ styrene acrylic	Sialon, Maraging steels
	1050-1250	Achesons DAG 2626	Mar M246 up to 1150 °C
	800-1050	Borate glass + BN	Inconel M2213
Ti alloys	1010	Glass-Amlube 1000	Inconel
	1000	Glass-Deltaglaze FB414	Inconel
Cu alloys	450-950	Graphite	WC
	650-750	Synthetic graphite-grease mixture	H13 or H10A tool steel

lubricants can be applied to a particular situation. Table 1, gives work piece-tooling-lubricant combinations recommended for different temperatures (Ref 25). However, a particular combination need not be generically applied as the lubricants have overlapping operating temperature ranges as given in Table 2. So, the most important and well-known lubricants used in the hot forging industry are lubricant combinations, such as graphite, glass powder, mica, and mineral oils. Among these, the first three are reported to be the ones used for high strength alloys as well as Ni base superalloys (Ref 23-25). For the hot deformation conditions in this research, the lubrication requirements for the entire temperature range from 1100 to 1175 °C for Nimonic 115 superalloy were not available in the research of Lord and Loveday (Ref 25). Hence, combinations of lubricants having high temperature stability, namely graphite, glass, and mica were examined in this study. In forging of superalloys, prevention of cooling becomes essential when the ductility of the workpiece drops steeply below the hot forging

Table 2 Summary of lubricant types, applications, and trade names

Lubricant type	Form	Trade name	Temperature range, °C
PTFE (Teflon)	Spray film		Up to 200
Graphite	Foil	Rocal X2102	Up to 300
	Powder		650-750
Graphite in water	Liquid	Lubeserve Aquagraf B Amlube 235 Renite S-45/S-28 Acheson E.G 1403	RT-315
Graphite in alcohol	Liquid	Acheson DAG 580 Lubeserve PA580	250-300
Graphite/ molybdenum disulfide	Grease	Acheson DAG 1559	Up to 450
Molybdenum disulfide	Dry powder Liquid (in water)	Amlube 510 (powder) Amlube 555 (fluid)	Up to 400
Grease	Grease	Tallow fat Lithium 3 grease	400-450 650-750
Synthetic oil	Oil	Thermex 7015	400-450
Boron nitride	Liquid (in water)	Acheson DAG 5710	500-1000
Glass	Fluid	Amlube 1000 Amlube 1080	Up to 1010 Up to 1310

Table 3 Chemical composition of Nimonic 115* (wt.%)

Ni	Cr	Co	Ti	Al	Mo	Fe	C	Si	Mn	Zr	Cu
Bal.	14.34	13.3	3.79	4.98	3.26	0.3	0.14	0.14	0.08	0.057	0.02

*Ave. of at least three analyses

temperature range, so an insulating layer of mica, glass, and graphite reduces chilling. It was determined that through a combination of graphite powder, glass, and mica at both ends of the specimens, a controlled friction effect was achieved that gave the lowest flow stress values and minimized shearing and barreling of the specimens for the deformation processing conditions used in this work, as will be explained in the following sections. In general, the data are generated under different experimental conditions thereby making it difficult to conclude on the efficiency of one lubricant versus another. One of the objectives of this study is to evaluate under identical experimental conditions, the behavior of these lubricants.

5. Experimental Procedures

5.1 Materials

The dies were made of GTD-111 superalloy. The chemical composition of Nimonc 115 samples is given in Table 3. The ring specimens were machined and turned to 11 mm external diameter, 6 mm internal diameter, and 6 mm height, as shown in Fig. 3. Solution treatments were carried out on all samples before being used in the experiments. The specimens were heated to 1190 °C for 1.5 h, then furnace cooled to 1000 °C, and finally air cooled to room temperature.

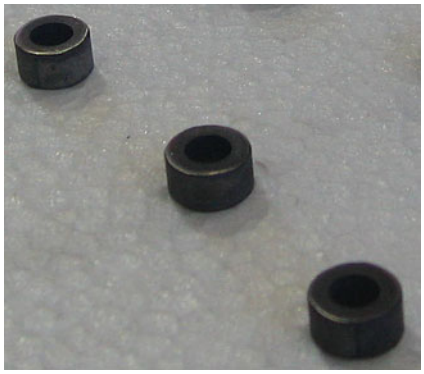

Fig. 3 Ring specimens

Fig. 4 Hot compression test machine

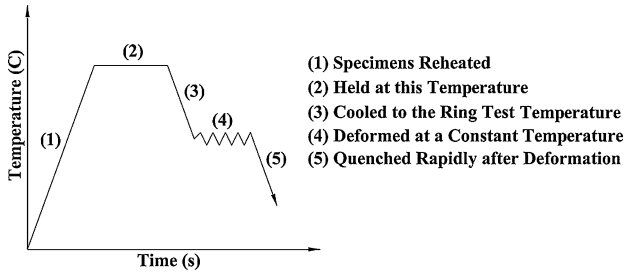

Fig. 5 Schematic diagram of hot compression test

5.2 Test Procedure

A computer-controlled, servo-screw type 250 kN Zwick/Roell testing machine was used for the hot ring compression experiments. It can be programed to simulate both the thermal and the mechanical industrial process variables for a wide range of hot deformation conditions, and is shown in Fig. 4.

Continuous hot ring compression tests were conducted at a strain rate of 1 s^{-1} at constant temperatures of 1100 and 1175 °C (shown schematically in Fig. 5).

Table 4 Chemical composition of glass powder

Composition	Wt.%	Composition	Wt.%
Na_2O	3.51	CeO_2	0.27
S	0.054	Al_2O_3	1.52
Cr_2O_3	0.009	CaO	1.32
ZnO	0.52	Fe_2O_3	0.42
MoO_3	0.035	SrO	7.7
Sb_2O_3	0.49	CdO	0.016
La_2O_3	0.052	HfO_2	0.039
MgO	0.57	SiO_2	54.1
K_2O	6.1	TiO_2	0.44
MnO	0.012	NiO	0.011
Ga_2O_3	0.007	ZrO_2	2
PdO	0.37	In_2O_3	0.18
BaO	9.4	PbO	10.9

Table 5 Chemical composition of mica plate

Composition	Wt.%	Composition	Wt.%
Na_2O	0.24	Al_2O_3	33.9
SO_3	0.016	K_2O	11.1
TiO_2	0.62	Fe_2O_3	4.8
ZnO	0.011	GeO_2	0.0017
SrO	0.0019	Nb_2O_5	0.031
BaO	0.0058	L.O·I	4.2
MgO	0.33	SiO_2	44.3
Cl	0.028	CaO	0.015
MnO	0.043	CuO	0.0016
Ga_2O_3	0.013	Rb_2O	0.16
ZrO_2	0.0016	SnO_2	0.024
La_2O_3	0.072	...	...

The experiments were completed with four different forms of lubrication:

1. Graphite powder
2. Glass powder
3. Mica plate
4. Dry

A lubricant covered all surfaces of a specimen, except for mica plate which was applied only on the active end surfaces of the specimen. The chemical compositions of the glass and mica lubricants used in the present investigation are given in Table 4 and 5, respectively. The hot ring compression was performed with 24 specimens at three different height reductions (25, 40, and 55% reduction).

5.3 Material Behavior

During hot deformation of the workpiece, strain, strain rate, and temperature have a great influence on the flow and behavior of the material, which can be expressed as the equation:

$$\sigma = \sigma(\varepsilon, \dot{\varepsilon}, T) \quad \text{(Eq 10)}$$

In this paper, the material flow behavior can be realized by inputting the flow stress data, gained in the thermo-mechanical simulation experiments. Stress-strain responses of

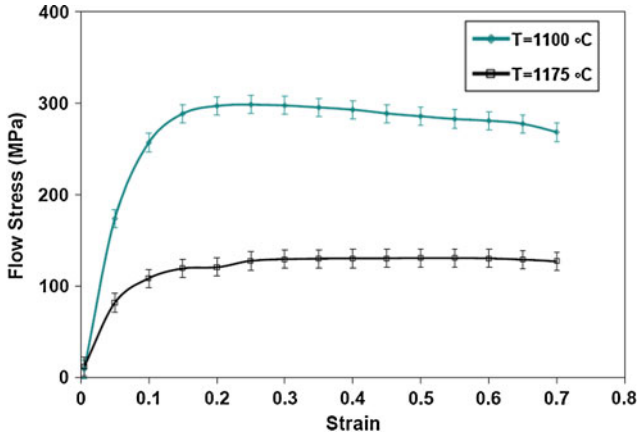

Fig. 6 Flow stress curves under different temperatures

Fig. 7 The measurement technique by profile projector

the materials were measured in several uniaxial compression tests on circular cylindrical specimens. Figure 6 shows the flow stress curves under different temperatures at constant strain rate of 1 s^{-1}.

5.4 Dimension Measurement

The accuracy in the measurements of the specimen dimensions before and after testing has a significant effect on the accuracy of the results of ring compression tests. Measurements of height and internal diameter (ID) were made utilizing digital calipers and micrometer, whereas details of the geometrical profile of the deformed specimens were obtained on a profile projector equipped with an *X-Y* micrometer table connected to a PC-based data-logging system (Fig. 7). Furthermore, the method devised for measuring the ID of the specimens involves placing a ball-bearing of known diameter onto the specimen so that it projects slightly into the inner hole, as depicted in Fig. 8. From the dimensions shown in Fig. 8, all of which can be measured accurately (±0.01 mm) using a standard micrometer, the ID is simply calculated from:

$$\mathrm{ID} = 2\sqrt{\frac{D^2}{4} - \left(OH - h - \frac{D}{2}\right)^2} \qquad \text{(Eq 11)}$$

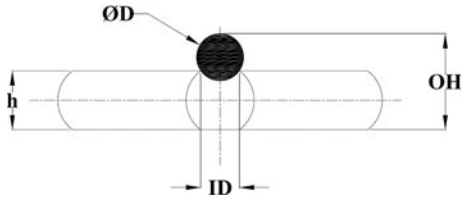

Fig. 8 Diagram illustrating the measurement technique used, showing the cross section of the deformed sample with ball in place

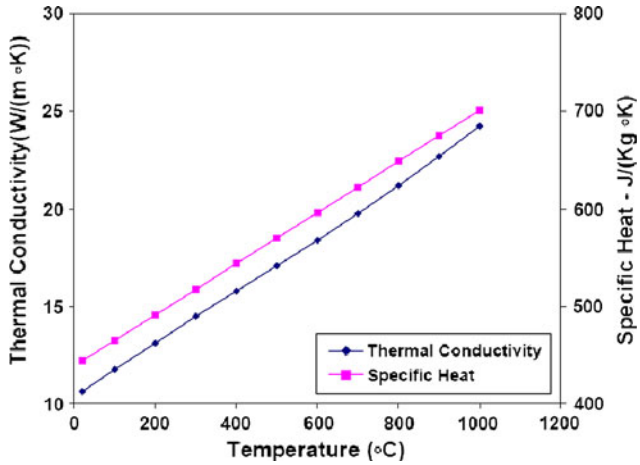

Fig. 9 Thermal physical properties curves under different temperatures

6. Finite Element Simulation

The friction calibration curves were derived using a FEM simulation. The simulations have been made using a thermal mechanical coupled analysis, where all material data are given as function of the temperature (Fig. 6). This was carried out to model the dimensional changes of the inner diameter corresponding to height reduction under different friction conditions. FEM simulations also provided detailed information on the ring deformation, so that a comparative study between FE simulations and experiments of the ring compression tests may be possible. The friction factor "*m*" at the workpiece and tool interfaces can then be calculated from the stress tensors using the law of constant friction Eq. 5. The thermal physical properties of specimens are given in Fig. 9.

The same material properties were used as for the analysis of the ring compression of the specimens. In FEM modeling, the top and bottom dies were represented as rigid. During ring compression tests, the bottom die speed changes with the ram movement of the press, which can significantly affect the average strain rate. The velocity of the moving ram was kept constant, producing on average strain rate of 1 s^{-1}. Figure 10 illustrates the stages of deformation during ring compression test simulation. In the finite element discretization, the sample was divided into 18,563 elements and 4472 nodes.

7. Results and Discussion

The deformed rings for each lubricant at two different temperatures (1100, 1175 °C) from the experiments are shown

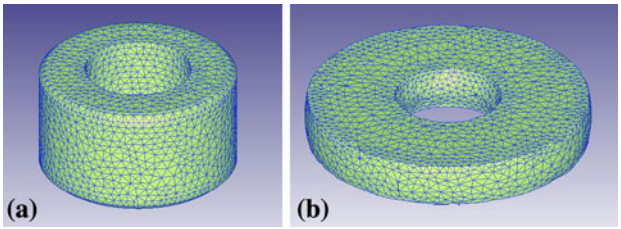

Fig. 10 FEM simulation of the ring compression test. (a) Undeformed elements; (b) deformed elements, 60% reduction in height

(a) Graphite; T=1100 °C

(b) Graphite; T=1175 °C

(c) Glass; T=1100 °C

(d) Glass; T=1175 °C

(e) Mica; T=1100 °C

(f) Mica; T=1175 °C

(g) Dry; T=1100 °C

(h) Dry; T=1175 °C

Fig. 11 Samples of compressed rings using different lubricants at various temperatures; (a) graphite; T = 1100 °C; (b) graphite; T = 1175 °C; (c) Glass; T = 1100 °C; (d) glass; T = 1175 °C; (e) mica; T = 1100 °C; (f) mica; T = 1175 °C; (g) dry; T = 1100 °C; (h) dry; T = 1175 °C

in Fig. 11. The comparison of experimental and computed load versus stroke diagrams in Fig. 12 shows reasonable agreement.

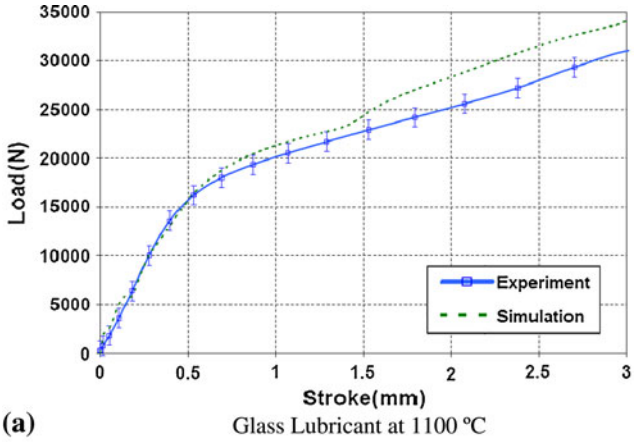

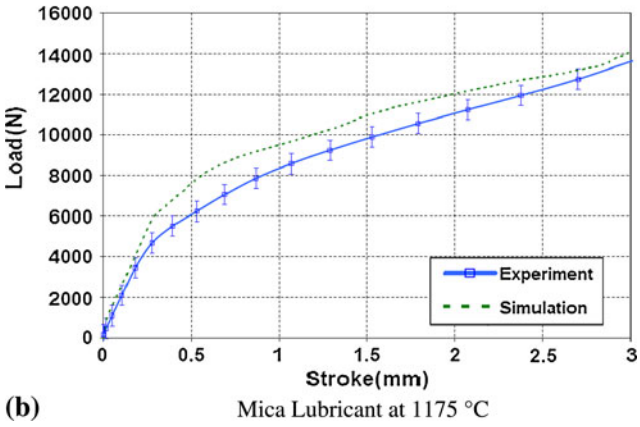

Fig. 12 Experimental and computed load-displacement curves of ring compression test; (a) glass lubricant at 1100 °C; (b) mica lubricant at 1175 °C

From the hot ring compression experiments and simulations, it is clear that the application of different lubricants at various temperatures produced different deformed profiles and surface roughness of the rings. When using lubricants with low friction coefficients such as Mica and glass, enlarged inner diameters of specimens were obtained, while reduced inner diameters were obtained for lubricants with high friction coefficients such as graphite and the dry condition, as shown in Fig. 11. Such dimensional changes of ring specimens are confirmed by the FE simulations. In Fig. 12, the load versus displacement data are shown for the two numerical simulations and for the experiments. The numerical values obtained with m = 0.307 and m = 0.313 are closer to the experimental data for glass lubricant at 1100 °C and mica lubricant at 1175 °C, respectively.

Based on the friction calibration curves derived from FEM simulations and the hot ring compression experiments, friction coefficients for different lubricants at various temperatures were obtained as shown in Fig. 13. Mica plate has friction coefficients of m = 0.289, m = 0.313 at temperatures 1100 and 1175 °C, respectively. Glass powder has higher values of m = 0.307 and m = 0.381 at these temperatures. In the case of graphite, a higher friction condition was observed at above mentioned temperatures (m = 0.499, 0.601), respectively. But the dry condition gave friction coefficients of m = 0.528 and m = 0.851 at temperatures of 1100 and 1175 °C, respectively. Therefore, the case of mica used in the hot ring compression tests for Nimonic 115 superalloy at elevated temperatures

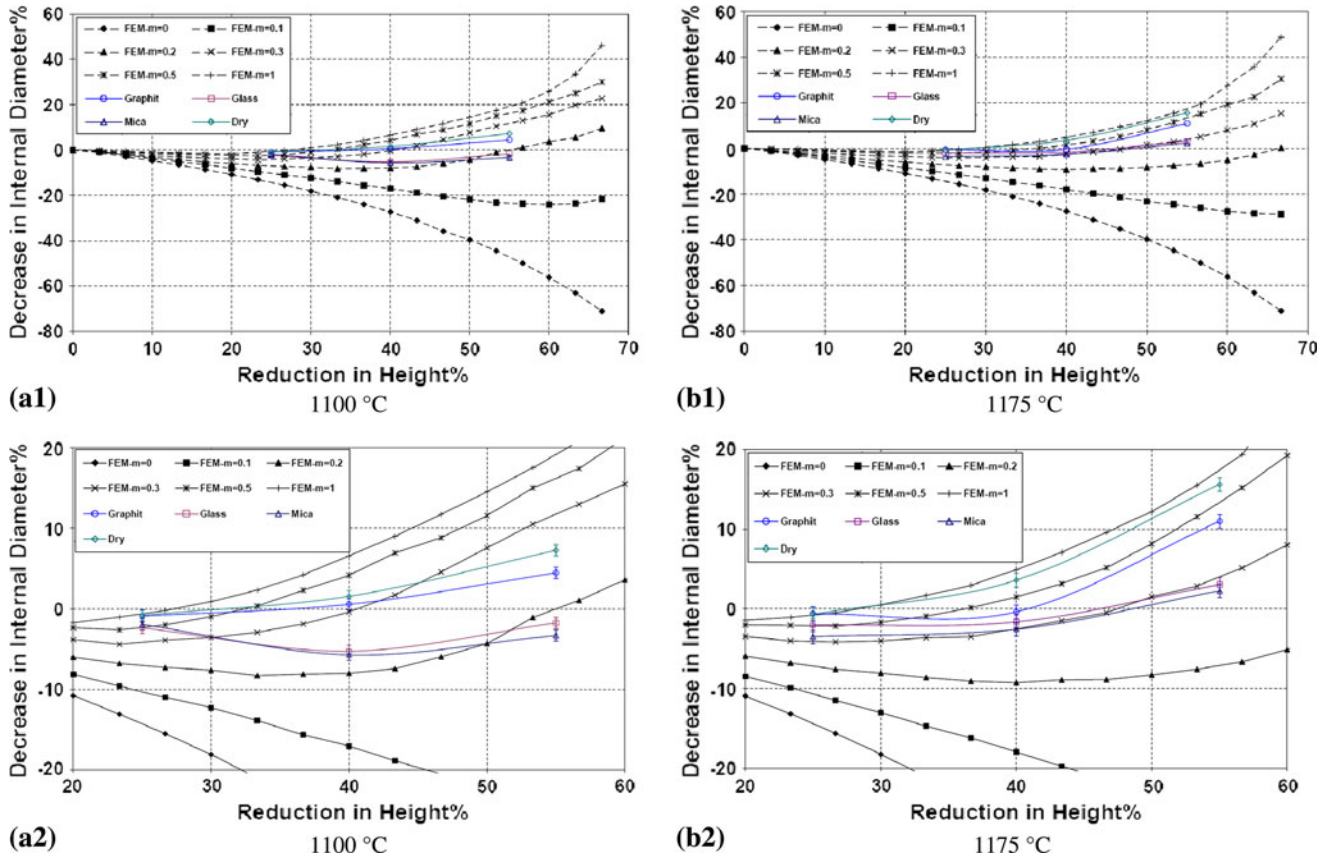

Fig. 13 Friction calibration curves and experimental results at different temperatures; (a) 1100 °C, (b) 1175 °C

Table 6 Corresponding average friction factors for the applied lubricants

	Mica	Glass	Graphite	Dry
m	0.30	0.35	0.55	0.69
μ	0.16	0.18	0.28	0.34

provided best lubrication. The average values of "*m*" and the corresponding "μ" values are given in Table 6. The current results show that for the dry condition where the test temperature is 1100-1175 °C, interfacial friction strongly increases with temperature. It was observed the friction coefficient "*m*" increases to nearly full sticking. This is evidenced in Fig. 14, giving temperature versus friction factor. The present investigation has also shown the temperature variations have no strong effects on the friction factor of mica lubricant. The friction coefficients remain nearly constant for the mica lubricant.

Within this range of temperature, the graphite lubricant behaves as a solid, so shearing would occur in the lubricant film. The shear strength of a lubricant film τ_s was observed to vary with temperature as follows:

$$\tau_s = \tau_0 \exp\left(-\frac{Q}{RT}\right) \quad \text{(Eq 12)}$$

where τ_0, Q, R are a constant, the activation energy (negative value), and the universal gas constant, respectively.

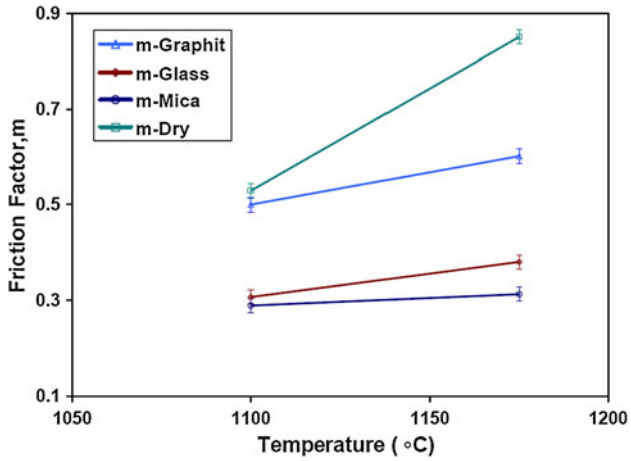

Fig. 14 Dependence of the friction factor on the temperature using different lubricants

When the shear strength of the lubricant (τ_s) decreases with the increase of temperature, the interfacial friction factor decreases simultaneously. Mica may be regarded as an inorganic thermoplastic polymer of a spatial network structure. On cooling from a high temperature at the usual rate, its viscosity increases sufficiently for it to behave like a solid, yet without acquiring a crystalline structure. It is similar to a Newtonian liquid. It has no boundary lubrication properties and

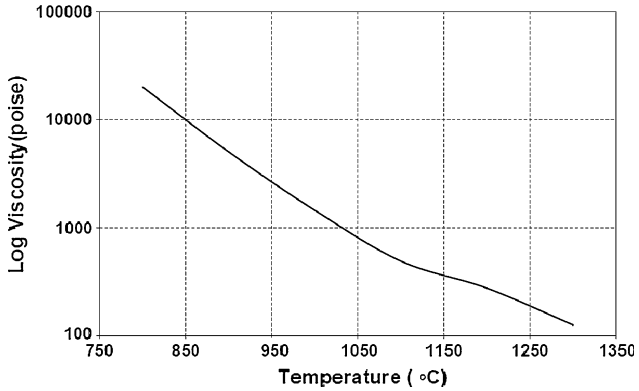

Fig. 15 Variation of viscosity with temperature for typical glass lubricant

therefore its most important property is viscosity. The viscosity decreases with the temperature according to an exponential law:

$$\eta = A \exp\left(\frac{E}{RT}\right) \quad \text{(Eq 13)}$$

where A is a constant, E is the activation energy, and R is the universal gas constant.

The viscosity of a typical glass lubricant at different temperatures is presented in Fig. 15 (Ref 23, 26). It can be seen that the shear strength of the glass and mica lubricants is directly proportional to viscosity. Therefore with the decrease of glass and mica lubricants viscosity, its shear strength and friction factor decrease. At high temperatures, the mica lubricant possesses liquid characteristics. At a strain rate of 1 s^{-1}, there is not sufficient time for the lubricant to be squeezed out, resulting in favorable lubrication conditions and low values of m, as shown in Fig. 13 and 14. However, when glass or graphite lubricant is used at temperatures higher than 1100 °C, the deformation strain rate could be adjusted even higher than 1 s^{-1} value to potentially reduce friction. Due to the existence of the effects of other parameters, it is not possible to introduce a suitable equation to express the relationship between the friction factor "m" and the temperature at the present strain rate.

8. Conclusions

Based on the findings presented in this study, the following conclusions are made:

(a) Using the ring compression experiment results, it is recommended to carry out the hot forging process of Nimonic 115 with mica, glass, and graphite as a lubricant, listed in order of decreasing performance and increasing friction coefficient.
(b) The mica plate is an excellent lubricant for hot forging of Nimonic 115, as increasing the temperature causes the friction coefficient to be nearly constant and its value is approximately 0.3.
(c) The value of friction coefficient increases with an increase in temperature.
(d) Under the dry condition, the friction coefficient in hot forging process is high, near 0.7.
(e) With increasing friction coefficient, the adhesion of dies and specimen increases.
(f) Flow stress curves indicated that the optimum hot ductility of Nimonic 115 was observed at temperature 1175 ± 5 °C at the strain rate of 1 s^{-1}.

Acknowledgments

The authors sincerely thank Prof. M. Jahazi, Prof. A. Akbarzadeh, Prof. M.J. Nategh, Dr. G. Ebrahimi, and Engineer M. Cheraghzadeh for their valuable assistances in this research. The present investigation has been carried out with the financial support of Mapna group-Mavadkaran Eng. Co.

References

1. M.J. Donachie and S.J. Donachie, Chap. 1, 3, 6, *Superalloys a Technical Guide*, ASM International, Materials Park, OH, 2002
2. C.T. Sims, N.S. Stoloff, and W.C. Hagel, Chap. 3, 4, 9, 16, *Superalloy II*, Wiley, New York, 1987
3. N.K. Park, I.S. Kim, and Y.S. Na, Hot Forging of a Nickel-Base Superalloy, *J. Mater. Proc. Technol.*, 2001, **111**, p 98–102
4. G. E. Dieter, Chap. 1, 4-6, 8, *Workability Testing Techniques*, American Society for Metals, Metals Park, OH, 1984
5. T. Altan, G. Ngaile, and G. Shen, Chap. 1-9, 11, 20, *Cold and Hot Forging*, ASM International, Materials Park, OH, 2004
6. A.T. Male, Variations in Friction Coefficients of Metals During Compressive Deformation, *J. Inst. Metals*, 1966, **94**, p 121–125
7. A.T. Male, The Effect of Temperature on the Frictional Behavior of Various Metals During Mechanical Working, *J. Inst. Metals*, 1965, **93**, p 489–494
8. S.C. Jain and A.N. Bramley, Speed and Frictional Effects in Hot Forging, *Proc. Inst. Mech. Eng.*, 1968, **182**, p 783–798
9. A.T. Male, V. Depierre, and G. Saul, The Relative Validity of Concept of Coefficient of Friction and Interface Friction Shear Factor for Use in Metal Deformation Studies, *ASLE Trans.*, 1973, **16**, p 177–184
10. E. Felder and J.L. Montagut, Friction and Wear During the Hot Forging of Steels, *Tribol. Int.*, 1980, **13**(2), p 61–68
11. O. Pawelski, W. Rasp, and C. Hoerster, Ring Compression Test as Simulation Test for the Investigation of Friction in Hot Metal Forming, *Steel Res.*, 1989, **60**(9), p 395–402
12. S. Venugopal, G. Srinivasan, S. Venkadesan, and V. Seetharaman, A Note on the Determination of the Friction Factor by Means of the Reduction-Capacity Test, *J. Mech. Work Technol.*, 1989, **19**, p 261–266
13. M.H. Sadeghi and T.A. Dean, Analysis of Ejection in Precision Forging, *Int. J. Mech. Tools Manuf.*, 1990, **30**(4), p 509–519
14. R.L. Goetz, V.K. Jain, J.T. Morgan, and M.W. Wierschke, Effects of Material and Processing Conditions Upon Ring Calibration Curves, *Wear*, 1991, **143**(1), p 71–86
15. F. Wang and J.G. Lenard, An Experimental Study of Interfacial Friction-Hot Ring Compression, *J. Eng. Mat. Technol.*, 1992, **114**(1), p 13–18
16. N.T. Rudkins, P. Hartley, I. Pillinger, and D. Petty, Friction Modelling and Experimental Observations in Hot Ring Compression Tests, *J. Mater. Proc. Technol.*, 1996, **60**, p 349–353
17. H. Sofuoglu and J. Rasty, On the Measurement of Friction Coefficient by Utilizing the Ring Compression Test, *Tribol. Int.*, 1999, **32**(6), p 327–335
18. C.D. Lee, C.I. Weng, and J.G. Chang, A Prediction of the Friction Factor for the Forging Process, *Metall. Trans. B*, 2001, **32**(B), p 137–143
19. S. Kobayashi, S.I. Oh, and T. Altan, Chap. 1-9, 12, 14, *Metal Forming and the Finite Element Method*, Oxford University Press, New York, 1989
20. A. Stuzalec, Chap. 1-6, 9-13, 15, 16, *Theory of Metal Forming Plasticity Classical and Advanced Topics*, Springer, Berlin, Germany, 2004

21. E.M. Mielnik, Chap. 1-4, *Metal Working Science and Engineering*, McGraw-Hill, New York, 1991
22. B. Avitzur, Forging of Hollow Discs, *Israel J. Technol.*, 1964, **2**(3), p 295–304
23. J.A. Schey, Chap. 1-5, 9, *Tribology in Metal Working: Friction, Lubrication and Wear*, ASM International, Metals Park, OH, 1983
24. G.E. Cheng, *ASM Handbook*, vol. 18, 9th ed., ASM International, Warrendale, PA, 1999, 79 pp
25. J.D. Lord and M.S. Loveday, *Tools and Lubricants for High Temperature Metalworking Laboratory-Scale Tests*, Centre for Materials Measurement and Technology, National Physical Laboratory, Queens Road, Teddington, Middlesex, UK TW110LW, CMMT (MN) 050, March 2001
26. J.F. Shackelford and W. Alexander, Chap. 1, 2, 5, 6, *Material Science and Engineering Handbook*, CRC Press, New York, 2001